

A Numerical Study of the Damage Mechanisms of the Specimens (SENT, SENB, CT, and DENT) used for P265 GH steel

Mohammed Lahlou *

•

Chouaib Doukkali University of El Jadida, Natl Sch Appl Sci, Sci Engineer Lab Energy, El Jadida, Morocco, lahloumohammed89@gmail.com

Bouchra Saadouki

•

Laboratory of Control and Mechanical Characterization of Materials and Structures, National Higher School of Electricity and Mechanics, BP 8118 Oasis, Hassan II University, Casablanca, Morocco, bouchra.saadouki@gmail.com

Abderrazak En-naji

•

Department of Physics, Laboratory M3ER, Faculty of Sciences and Technology, Moulay Ismail University, Meknes, Morocco, abdenaji14@gmail.com

Fatima Majid

•

Laboratory of Nuclear, Atomic, Molecular, Mechanical and Energetic Physics, University Chouaib Doukkali, El jadida, Morocco, majidfatima9@gmail.com

Nadia Mouhib

•

Higher Institute of Maritime Studies ISEM, Casablanca, Morocco
mouhib.nadia@gmail.com

Abstract

During operation, most mechanical structures are subjected to time-varying stresses, which leads to their failure of serious accidents. The lifetime of a mechanical structure is broken down into three stages: stage I; the initiation, stage II; the slow propagation and stage III; the brutal propagation. The objective of this paper is to determine the damage and the lifetime of a pressure equipment by establishing a numerical modeling by finite elements on different specimens (SENT, SENB, DENT, CT) using the calculation code CASTEM. The material studied is P265GH steel commonly used as boiler plate and pressure vessels. The results show that the damage severity of the SENT specimen is more important, followed by the DENT specimen, then the CT specimen and finally SENB.

Keywords: Pressure vessels; Finite element model; Mechanical behaviors; Damage; Tensile test; Maintenance.

1. Introduction

The computer has become an essential tool in our lives, specifically in the industrial sectors. For reasons of competitiveness and development, companies are looking to predict the durability and consider solutions in the design and maintenance of parts and structures. The finite element method can be used to solve these problems, more precisely mechanical problems [1].

All materials have defects on a microscopic scale (heterogeneities, inclusions, manufacturing defects, etc.), and all mechanical parts present section changes or rough surface states. Since these conditions favor the appearance of stress concentrations, we should often consider the possibility of crack initiation as well as its propagation when calculating a structure. For this reason, the designers of structures or any element subjected to cyclic loadings should not only take into account the possibility of cracking, but also estimate the velocity of crack propagation, to ensure that these cracks do not reach the critical length, which will inevitably lead to failure [2-7].

Behavior simulation with FEM has been presented by many authors with the aim of improving the knowledge of predicting trends. H. Yoshihara [8] presented the critical stress intensity factor on the SENT specimen. Saffih [9] studied the harmfulness of circumferential or axisymmetric semi-elliptical cracks in a cylindrical shell with a thickness transition. A. Hachim [10] presented a finite element based approach to simulate a Double Edge Notch Tension specimen of S355 Steel; he studied the behavior of the material in the presence of defects.

The finite element method adopted in this paper is the most commonly used for real applications to provide a robust solution for most industrial problems.

This work is based on the finite element analysis of various specimens (SENT, SENB, DENT, CT) using the calculation code CASTEM to classify the criticality of these specimens.

2. Expérimentation

To extract the mechanical characteristics of the P265GH steel used in our program, tensile tests on standard specimens (Figure 1) were conducted in different directions of roll (longitudinal and transversal) [11]. The test curves showing the stress versus strain are given in figure 2.

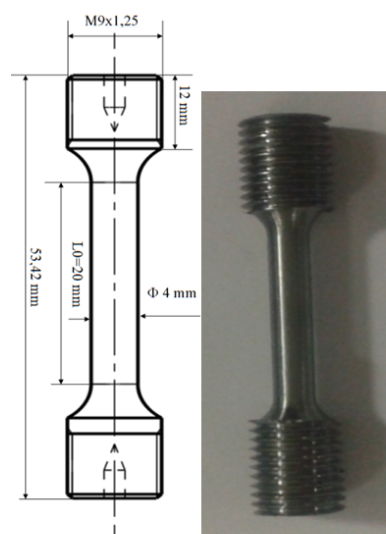


Figure 1 : Dimensions of the tensile test specimen

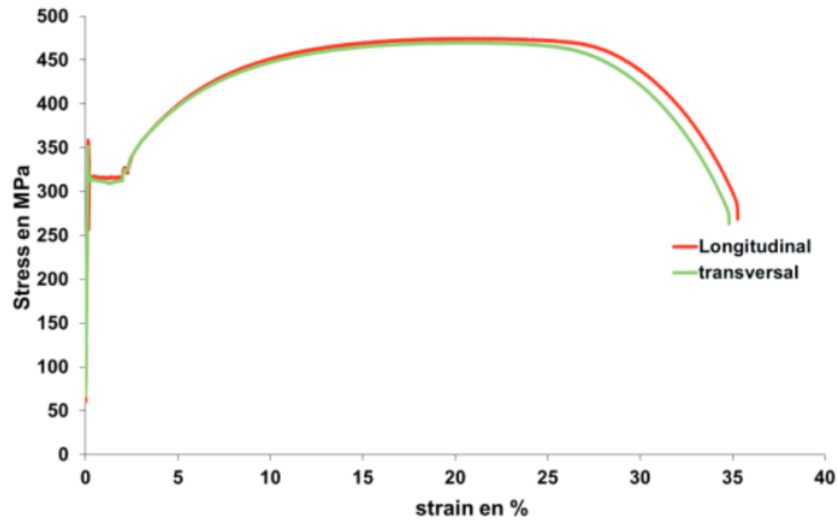


Figure 2 : Traction curve

By comparing the mechanical characteristics of specimens in both rolling directions, it is found that there is a negligible difference between tensile test curves. The mechanical characteristics of P265GH steel at the ambient temperature are reported in Table 1[12].

Table 1: Mechanical properties of the material

Young's modulus E (MPa)	elastic limit σ_e (MPa)	Breaking stress: σ_g (MPa)	Elongation %	Poisson's ratio ν
2.10^5	320	470	35	0,3

We notice that the elongation is about 35%, which is higher than the 14% required by the CODAP [13]. Therefore, this P265GH steel used is well adapted for pressurized structures.

3. Numerical modeling

The Cast3m [14] calculation code is used to create a finite element model for the analysis of the different specimens (SENT, SENB, DENT, CT).

3.1. Geometry

The geometries and dimensions of the specimens are shown in Figure 3. The study is restricted to mode I.

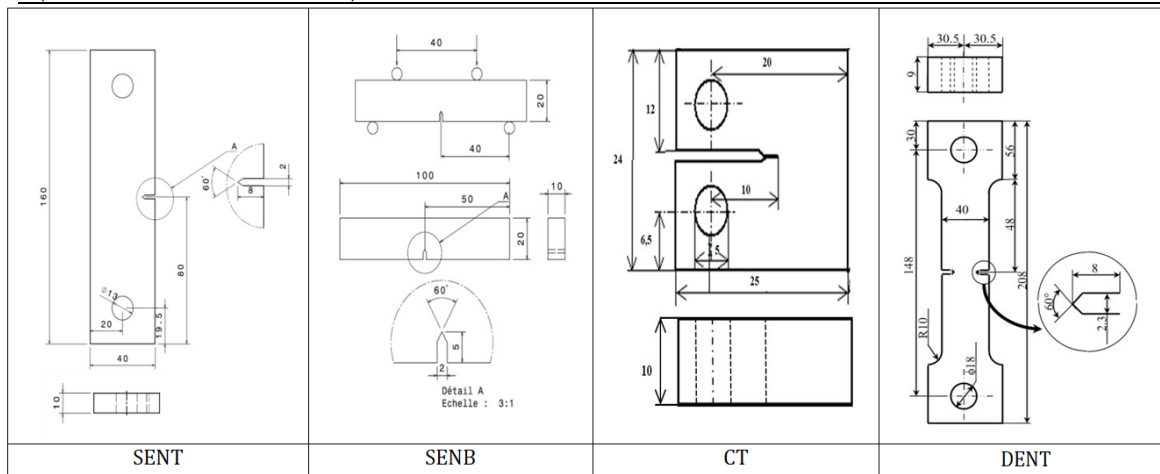


Figure 3 : The geometry of the specimens

3.2. Mesh, boundary conditions and Loading

For the DENT specimen, there are two planes of symmetry. Therefore, only a quarter of this specimen is modeled [15]. On the other hand, for the specimens (SENT, CT, and SENB), only one plane of symmetry appears, so half of the parts are modeled.

The numerical results are intended for analysis of fracture mechanics. Special attention is paid to mesh principally in the crack and its vicinity (Mesh Refinement using Barsoum elements) [16]. Details of the mesh are illustrated in figure 4.

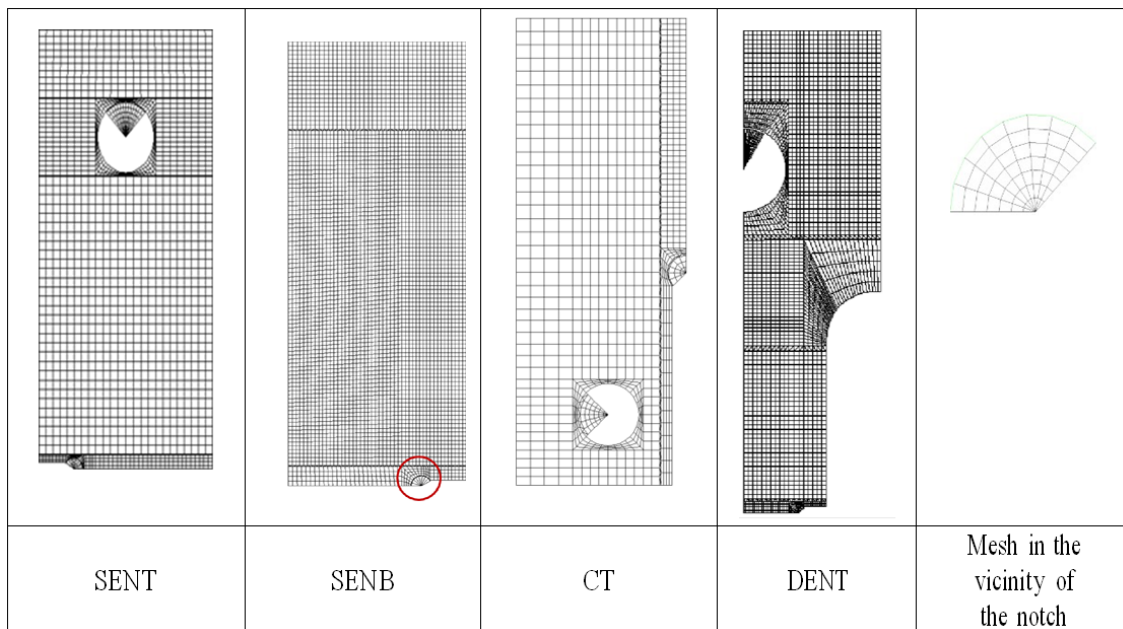


Figure 4 : The mesh of test pieces

4. Results and discussion

For all specimens, the life fraction (β) is the notch length over the specimen width ($\beta=a/w$) [17]. For each notch depth, we determine the stress that leads to failure. This stress is called the ultimate residual stress (σ_{ur}). And (σ_u) is the value of the ultimate stress in the initial state;

The curves in Figure 5 show the evolution of the dimensionless stress [18] (σ_{ur} / σ_u) as a function of the life fraction for the SENT, DENT, SENB, and CT specimens.

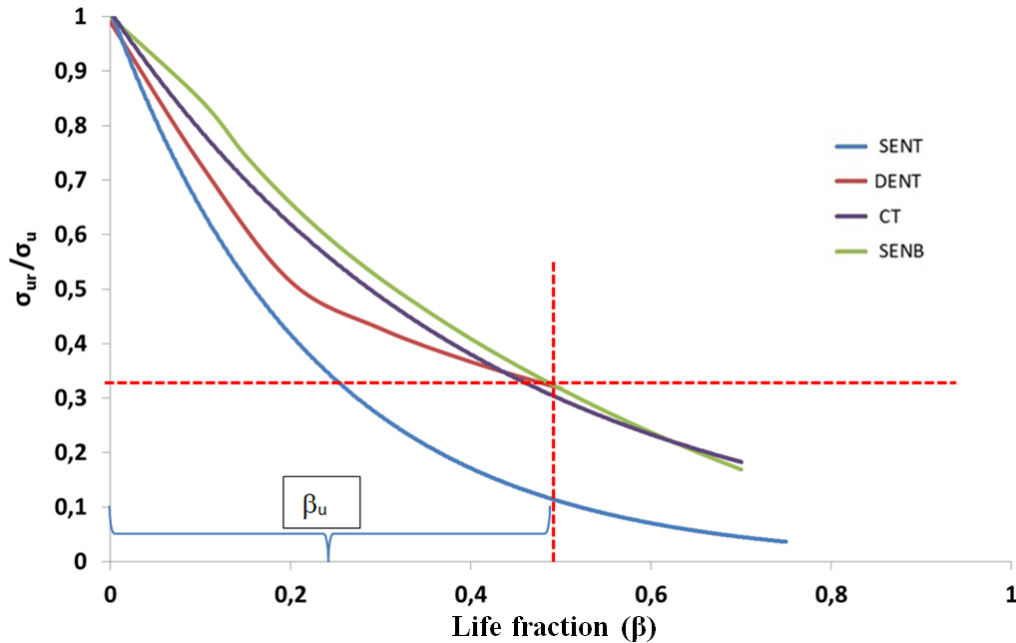


Figure 5 : Dimensional stress as a function of life fraction for SENT, DENT, SENB and CT specimens

The analysis of the curve in Figure 5 shows that the dimensionless stress decreases as a function of the fraction of life. We note that the stress loss is very aggressive for the SENT specimen, followed by the DENT specimen, the CT specimen, and finally the SENB specimen.

We also note that, from life fraction, the dimensionless stress of all specimens is less than 33% (a safety factor equal to 3). Therefore, we define the useful life fraction ($\beta_u=a/w_u$) as the ratio of the notch length and the width of the useful specimens (with a safety factor equal to 3).

4.1. Quantification of the static damage

The static damage model is based on the residual stress evolution according to the equation (1) [19,20].

$$D = \frac{1 - \frac{\sigma_{ur}}{\sigma_u}}{1 - \frac{\sigma_a}{\sigma_u}} \quad (1)$$

with:

- σ_u : Value of the ultimate stress in the initial state ;
- σ_{ur} : Value of the residual ultimate stress ;
- σ_a : Stress just before break in the useful zone.

The boundary conditions are shown below:

$$\begin{array}{l} \text{In the initial state} \\ \text{In the final state} \end{array} \quad \begin{array}{l} \beta_u = 0 \rightarrow \\ \beta_u = 1 \rightarrow \end{array} \quad \begin{array}{l} \sigma_{ur} = \sigma_u \rightarrow D = 0 \\ \sigma_{ur} = \sigma_a \rightarrow D = 1 \end{array}$$

The variation of damage as a function of useful life fraction β_u for the specimens (SENT, DENT, SENB, and CT) is illustrated by the curves in Figure 6:

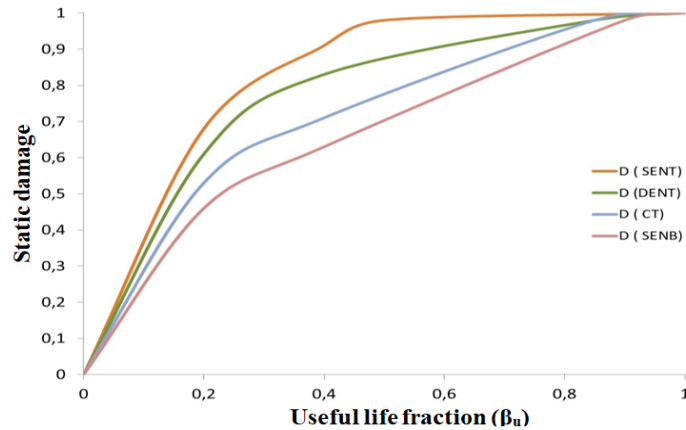


Figure 6 : Static damage to residual stress as a function of the useful life fraction

The increase in damage causes an increase in the static tensile strength loss of the specimens. From the curves in Figure 6, we observe that the damage evolution of the tensile specimen (SENT) is the most critical for the same fraction of service life (β_u), while the damage of the bending specimen (SENB) is the less critical.

Reliability is the inverse of damage, and equation (2) shows the ratio between damage and reliability [21]:

$$R(\beta_u) + D(\beta_u) = 1 \tag{2}$$

The equation obtained is used to draw the curve of the reliability variation with the damage curve (Figure 7) for the SENT, DENT, CT, and SENB specimens.

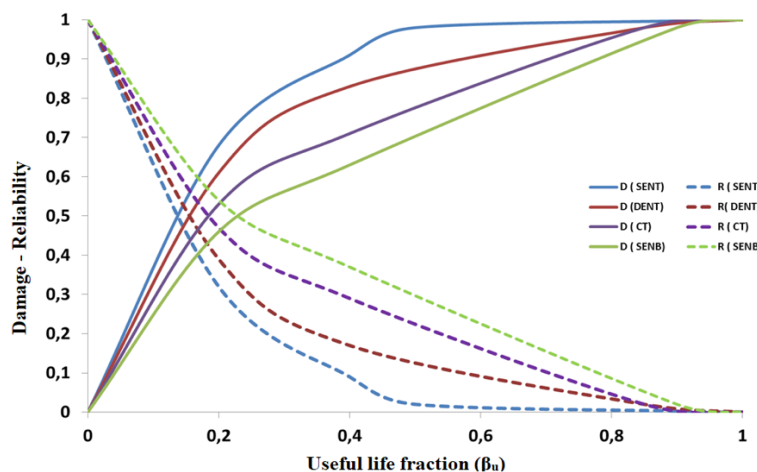


Figure 7 : Damage - Reliability as a function of the usual life fraction

The Reliability-Damage curves for each specimen intersect at a β_{ui} intersection point. This point of intersection is coincident with a reversal of the situation. Indeed, the reliability that was initially higher than the damage decreases beyond this point. This corresponds to the acceleration of damage. The damage becomes critical and uncontrollable when the damage value exceeds 80%, this value is named the critical life fraction β_{uc} .

Damage is generally described by the following three stages:

- Stage I [0, β_{ui}]: Corresponds to the initiation of damage where reliability is higher than damage.
- Stage II [β_{ui} , β_{uc}]: Corresponds to progressive damage where predictive maintenance is required.
- Stage III [β_{uc} , 1]: Corresponds to the brutal damage. At this stage of damage, the specimen is declared failed.

The table 2 recapitulates the stages of damage and the criticality of the damage for each of the specimens studied.

Table 2: Damage stage results

Specimens	SENT	DENT	CT	SENB
Stage I	[0, 0,16]	[0, 0,17]	[0, 0,19]	[0, 0,22]
Stage II	[0,16, 0,27]	[0,17, 0,35]	[0,19, 0,53]	[0,22, 0,63]
Stage III	[0,27, 1]	[0,35, 1]	[0,53, 1]	[0,63, 1]
Criticality of the damage	Important	Less important	Moderate	Minimal

4.2. Quantification of damage by unified theory

The loading level applied on the material influences the progression and the behavior of its damage. The various theories representing this damage are given by the linear model initiated by Miner's law according to which the damage evolves linearly as a function of the life fraction.

By analogy, with the unified theory, an empirical relation describing the damage is proposed (equation (3)) [22]:

$$D_{th} = \frac{\beta_u}{\beta_u + (1 - \beta_u) \left[\frac{\gamma - (\frac{\gamma}{\gamma_u})^\beta}{\gamma - 1} \right]} \quad (3)$$

With

$$\beta_u = \frac{a}{w_u}, \gamma = \frac{\sigma_{ur}}{\sigma_0} \text{ and } \gamma_u = \frac{\sigma_u}{\sigma_0}$$

$$\sigma_0 = \alpha \sigma_u \text{ is the endurance limit of the virgin material, with } \alpha = \frac{1}{\text{factor of safety}} = 0.33$$

In this unified theory, many curves are drawn. Each curve is associated with a loading level defined with σ_a .

Figure 8 show the damage curves by the unified theory for the specimens SENT, DENT, CT, and SENB:

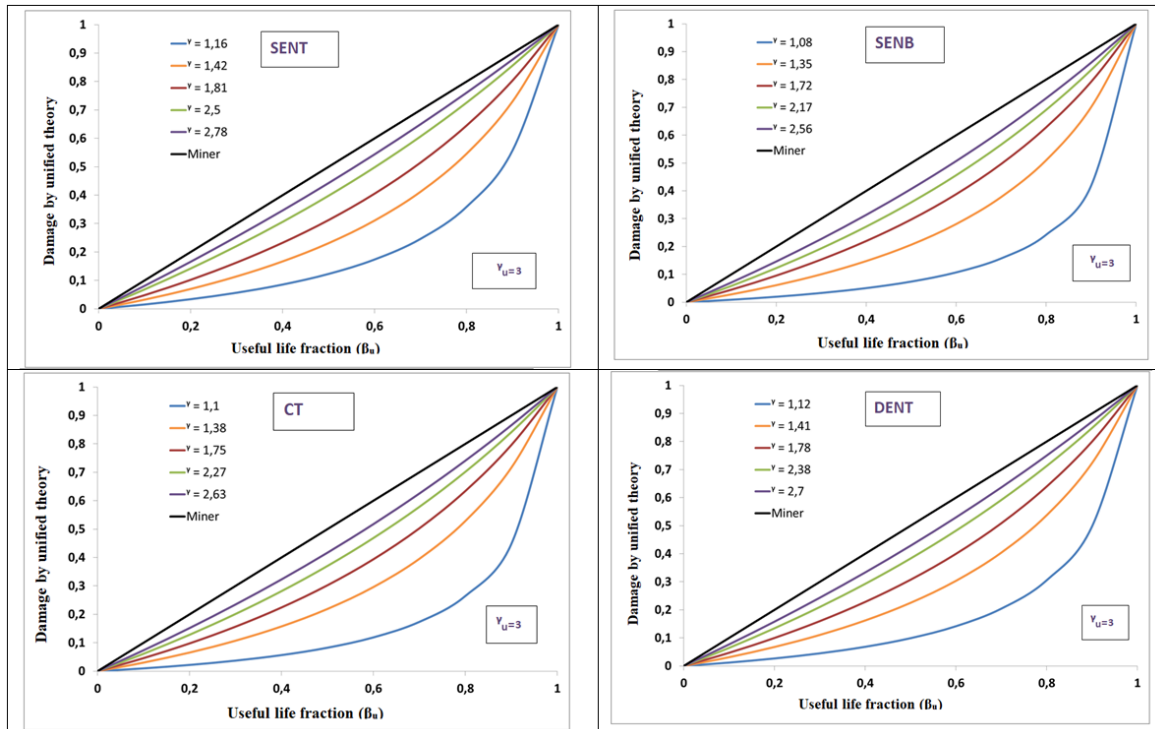


Figure 8 : Evolution of Damage by unified theory and Miner law in function of the life fraction

The analysis of the curves shows that the damage curve is gradually approaching the bisector (Miner's linear rule) as a function of βu for high loading levels.

The damage curves by unified theory are below the Miner's law curve. Therefore, Miner's law presents more simplicity to the user than the unified theory. For this reason, many researchers adopted this law for the study of damage.

5. Conclusion

In risky structures such as pressure equipment and in the presence of cracks, for safety reasons, it is fundamental to know precisely the degree of damage of the failure. Numerical modeling by the finite element method is a very effective tool to resolve this problem. The analysis of the results shows that the damage evolution of the tensile specimen (SENT) is the most critical for the same fraction of life, while the damage of the bending specimen (SENB) is the less dangerous.

References

- [1] Lahlou, M., Hachim, A., Mouhib, N., Ouaoumar, H., Rachik, M., & El Ghorba, M. (2015). Numerical modeling and analytical validation of stress intensity factor and crack velocity for SENT tensile specimen of. *International Journal of Research*, 2(6), 489-494.
- [2] Damien Fournier, (2011) *Analyse et Développement de Méthodes de Raffinement hp en Espace pour l'Equation de Transport des Neutrons*, Mémoire de thèse doctorat Université de Provence Marseille,
- [3] LAHLOU, M., et al. "Numerical modeling and analytical validation of stress and stress intensity factor for SENT tensile specimen of P265GH steel material." *IPASJ International Journal of Mechanical Engineering (IJME)*: Volume 3, Issue 4, April 2015 pp. 042-048
- [4] Zekriti, Najat et al. "Mode I stress intensity factors of printed and extruded specimens based on Digital Image Correlation method (DIC): case of ABS material". *Procedia Structural Integrity*. 28. 1745-1754. (2020). DOI : 10.1016/j.prostr.2020.10.149.
- [5] Majid, Fatima et al. "Mechanical behavior and crack propagation of ABS 3D printed specimens". *Procedia Structural Integrity*. 28. 1719-1726. (2020). DOI : 10.1016/j.prostr.2020.10.147.
- [6] En-Naji, Abderrazak & Lahlou, M. & Ghorba, M. & Mouhib, Nadia. "Change of experimental elongations with increasing temperature for an abs material subjected to tensile test". *International Journal of Mechanical Engineering and Technology*. 9. 932-944.2018
- [7] Fatima Majid, Rajaa Rhanim, Mohammed Lahlou, Hassan Rhanim, Mohammed Ezzahi, Mohamed Elghorba, "Maintainability and reliability of high density polyethylene pipes through experimental and theoretical models", *Procedia Structural Integrity*, Volume 25, 2020, Pages 430-437, ISSN 2452-3216, <https://doi.org/10.1016/j.prostr.2020.04.048>
- [8] Yoshihara, H., 2013: "Mode II critical stress intensity factor of medium-density fiberboard measured by asymmetric four-point bending tests and analyses of kink crack formation". *BioResources* 8 (2): 1771-1789.
- [9] A. Saffih, S. Hariri, Numerical study of elliptical cracks in cylinders with a thickness transition, *International Journal of Pressure Vessels and Piping*, Vol 83, No. 1, pp. 35-41, 2006.
- [10] A. HACHIM, (2012) Numerical evaluation of stress triaxiality at the top of notch for a specimen steel notched bi-S355, *International Journal of Engineering and Science*, Vol. 1, Issue 1, PP 088-93
- [11] LAHLOU, M. et al. Numerical modeling and analytical validation of stress and stress intensity factor for SENB bending specimen of P265GH steel material. *International Journal of Research*, [S.l.], v. 2, n. 6, p. 468-472, jun. 2015.
- [12] CODAP: Code de Construction des Appareils à Pression non soumis à la flamme 2005
- [13] Lahlou, Mohammed et al. "Numerical Study of Internal Radius Effect on Mechanical Behavior of P265GH Material". *Periodica Polytechnica Mechanical Engineering*. 60. 233-237.(2016). DOI : 10.3311/PPme.8978.
- [14] LAHLOU, M., HACHIM, A., OUAOMAR, H., MOUHIB, N., & EL GHORBA, M. (2015). Procedure for the numerical modeling of the specimen (SENB) using CAST3M calculation code. *International Journal of Innovation and Scientific Research*, 19(2), 259-266.
- [15] Cast3M, code d'éléments finis, CEA. (Cast3M, finite element code.) [Online]. Available from: <http://www-cast3m.cea.fr/> [Accessed: 2013] (in French)
- [16] Barsoum, R. S. "Further application of quadratic isoparametric finite elements to linear fracture mechanics of plate bending and general shells." *International Journal of Fracture*. 11(1), pp. 167-169. 1975. DOI: 10.1007/BF00034724
- [17] N.MOUHIB "Static tests of a steel wire strand (1+6 wires) containing 3/7 damaged wires and prediction of its life time" *International Journal of Mechanical Engineering*, Vol3 (2015):pp.30-35.
- [18] M. LAHLOU, Etude numérique de l'endommagement des éprouvettes (SENT, SENB, CT et DENT) en acier P265GH, IXèmes Journées d'Etudes Techniques – JET'2016 Les 03, 04 & 05 Mai 2016, Hammamet – Tunisie
- [19] H.Ouaoumar, N. Mouhib, M. Lahlou, A .Barakat and M. El Ghorba ,Study of specific energy in elastic phase of the different elements of a low voltage underground power cable' *Int. J. Adv. Res. Sci. Technol*. Volume 4, Issue 6, 2015, pp.406-408.

[20] N.Mouhib, H.Ouaomar, M.Lahlou, M.Barakat and M. El Ghorba' Application of Student and Weibull statistical distributions on experimental tensile test results of steel wires extracted from antigyratory wire rope (19x7)'. *Int. J. Adv. Res. Sci. Technol.* Volume 4, Issue 6, 2015, pp.498-501.

[21] Mouhib, N., Ouaomar, H., Lahlou, M., & El Ghorba, M. 'Characterization of residual energy loss and Damage Prediction of 7-wire strand extracted from a steel wire rope and subjected to a static test' . *International Journal of Research*, 2015, vol. 2, no 6, p. 473-478.

[22] E. Boudlal, M. Barakat, N. Mouhib, M. Lahlou, M. El Ghorba, H. Ouaomar, "Mechanical Behaviour Of Damaged Central Core Strand Constituting A Steel Wire Rope Hoist Under The Effect Of A Static Load", *International Journal of Mechanical Engineering and Technology (IJMET)*, 2016, 7(3), PP.360-367